

## Correlating electrical properties and molecular structure of SAMs organized between two metal surfaces

Christian Grave<sup>a</sup>, Elizabeth Tran<sup>b</sup>, Paolo Samorì<sup>c</sup>, George M. Whitesides<sup>b</sup>, Maria A. Rampi<sup>a,\*</sup>

<sup>a</sup> Dipartimento di Chimica, Centro di Fotochimica CNR, Università di Ferrara, Via L. Borsari 46, 44100 Ferrara, Italy

<sup>b</sup> Department of Chemistry and Chemical Biology, Harvard University, Cambridge, MA 02138, USA

<sup>c</sup> ISOF-CNR, 40129 Bologna, Italy

Received 9 May 2004; received in revised form 29 June 2004; accepted 29 June 2004

### Abstract

We describe the results obtained on a series of junctions that are formed by mercury electrodes. The junctions comprise self-assembled monolayers (SAMs) sandwiched between two metal electrodes, i.e., metal (mercury)–SAM//SAM–metal (mercury, gold or silver) junctions. We describe three different variations on this type of Hg-based junction. The first junction, formed by bringing into contact two mercury drops covered by the same type of SAM, is a prototype system that provided useful information on the structure and electrical properties of the Hg-based junctions. The second junction consists of a Hg drop covered by one SAM (Hg–SAM(1)) in contact with a second SAM supported on a silver film (Ag–SAM(2))—i.e., a Hg–SAM(1)//SAM(2)–Ag junction. This junction (for constant SAM(1)) allowed systematic measurements of the current that flowed across SAM(2) as a function of its chemical structure. The same type of junction, when comprising a transparent solid metal electrode, allows to irradiate through the transparent surface photoactive units organized in a SAM and to measure the current photoresponse. The third type of junction, Hg–SAM//R//SAM–Hg (or Hg–SAM//SAM–Hg for redox-active SAMs), is an electrochemical junction that can (i) trap redox-active molecules (*R*) in the interfacial region between the SAMs and (ii) control the potential of the electrodes with respect to the redox potential of *R* using an external reference electrode. This junction becomes conductive when the electrode potentials are adjusted to the formal potential of the redox centers, and it shows diode- and transistor-like characteristics analogous to those of solid-state devices.

© 2004 Elsevier B.V. All rights reserved.

**Keywords:** Self-assembled monolayers; Molecular bridge; Metal surface; Molecular electronics; Electron transfer

### 1. Introduction

Investigations of electron-transfer processes have largely focused on the rates of transfer in solution between donor and acceptor species, either as separated entities or as separate sites of larger molecules [1]. Examinations of rates of electron transfer between covalently linked donor and acceptor units through a molecular bridge in species of the structure *D–B–A* (*D*: donor, *A*: acceptor, *B*: molecular bridge) have underlined the importance of the structure of the bridge in facilitating electron transfer from *D* to *A* (Fig. 1a). As a col-

loquial way to emphasize this role, it has been customary to refer to the bridge as a “molecular wire,” and to discuss its ability to “conduct” electrons. It is important to note that these “molecular wires”, while facilitating electron transport relative to vacuum, are not similar to metals either in the magnitude of their conductivity or in the mechanism of this conduction.

Most of our present understanding of electron transfer is based on measurements made in solution, but the conclusions from these studies do not necessarily hold for the same molecules in other environments (e.g., in the solid state). In his pioneering work in 1971, Mann and Kuhn contrasted electron-transfer studies in molecular systems in solution with electron transport in the solid state [2]; this work, for

\* Corresponding author. Tel.: +39 532 29 11 62; fax: +39 532 24 07 09.  
E-mail address: [rmp@unife.it](mailto:rmp@unife.it) (M.A. Rampi).

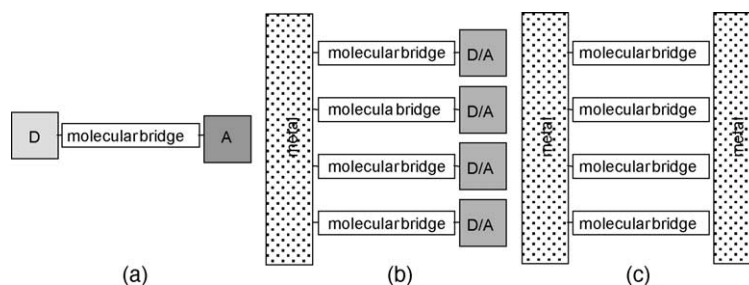


Fig. 1. (a) Sketches a  $D$ – $B$ – $A$  system. The process of the electron transfer from the donor ( $D$ ) to the acceptor ( $A$ ) site across the molecular bridge ( $B$ ) can be monitored in solution by time-resolved photophysical techniques. (b) Sketches an electroactive SAM on a metal surface. This system is made of a molecular bridge ( $B$ ), appropriately anchored to the metal surface, terminating with an electroactive group ( $D/A$ ). In such an arrangement, the use of fast electrochemical techniques can lead to the determination of heterogeneous electron-transfer rates from/to the metal surface to/from the electroactive group across the molecular wire. (c) Represents a metal–SAM–metal junction schematically; in this system, an array of molecules bridges two metal surfaces. In this type of experimental arrangement, the rates of electron transfer are measured as current density as a function of applied potential.

the first time, measured currents through molecular monolayers sandwiched between metal electrodes.

The use of molecular properties to make electronic devices was first envisaged by Aviram and Ratner [3] in a theoretical paper in 1974. Because there were no technologies that could establish electrical contacts across individual molecules, experimental investigations of the fundamental processes involved in electron transfer through molecules have focused on liquid-phase systems [1] (Fig. 1a). More recently, the well-defined structures of SAMs on metal electrodes have made it possible to study electron transport by electrochemistry [4–13] (Fig. 1b).

Only in the late 90s has the combination of nanotechnology [14], scanning probe microscopies [15], and methods to form electrically functional connections to metal surfaces [16] triggered the fabrication of metal–molecule(s)–metal junctions, and opened the door to experimental “molecular electronics” (Fig. 1c). Different type of junctions have been used to sandwich molecules (several, a few, or individual molecules) between two metal surfaces, and to measure their electrical properties [17–36].

The field is rapidly evolving, and a variety of different, often conceptually new junctions have been published. To name only a selection of the most recent ones, work has been done on methods to improve the critical fabrication of the second solid electrode on the organic layer by vapor deposition [37] or nanotransfer printing [38], junctions where the SAM covered metal electrodes (chips or wires) are brought into contact mechanically [39,40], capillary junctions [41], nanowire-based junctions [42], STM tip junctions [43–46], break junctions [47] or semiconductor-based junctions [48]. Junctions that include organic molecules of modest structural complexity [17,19,26,33,43,44,48,49] have showed properties that suggested that it may be possible to build devices that mimic the function of electronic components (conductors, transistors, rectifiers, logic gates).

Although informative  $i$ – $V$  characteristics for specific junctions have been identified and discussed, the factors influencing the electrical properties of metal–molecule(s)–metal junctions is still incomplete. The contributions of interfacial

processes relative to electron transport through organic material in determining conductivities remain unclear. As far as the mechanisms of transport of electrons through organic matter, while “through-bond tunneling” is the dominant mechanism in many cases, the presence of redox sites in the junction can switch the mechanism from tunneling to hopping [43,44,49].

Among the large number of junctions reported in the literature, each shows both advantages and limitations. We believe that it is important to provide a substantial body of experimental data as a foundation for research in molecular electronics, junctions are needed that are stable, reproducible, easy to assemble and to use, and broadly compatible with a range of organic structures.

## 2. Results and discussion

### 2.1. MIM junctions-based Hg electrode(s)

We have assembled, characterized, and studied different types of junctions, all using Hg-based electrodes (Fig. 2). They are easy to assemble (their assemble does not require sophisticated, expensive apparatus), stable and reproducible (only 20% of the junctions short or show anomalous conductivity), and versatile (they can host a large variety of molecules and molecular systems). Drops of Hg as electrodes provide four advantages: (i) the Hg surface, as a liquid, is free of structural features—edges, steps, terraces, pits—that result in defects of the adsorbed monolayer; (ii) Hg forms well-ordered SAMs after contact with alkanethiol-containing solutions for only a few seconds [8,50–53]; (iii) the Hg drop conforms to the topography of solid surfaces, and forms a good conformal contact with molecular monolayers on a solid surface; and (iv) the Hg drops form alkanethiolate SAMs that show liquid-like behaviors [8] (a SAM-covered drop of Hg is therefore able to conform to a solid surface without cracking the SAM). In addition, when the junction consists of a solid metal and a mercury electrode, each supporting a SAM, the chemical composition of the two SAMs can be different, and a variety of different metals can be used in the solid electrode

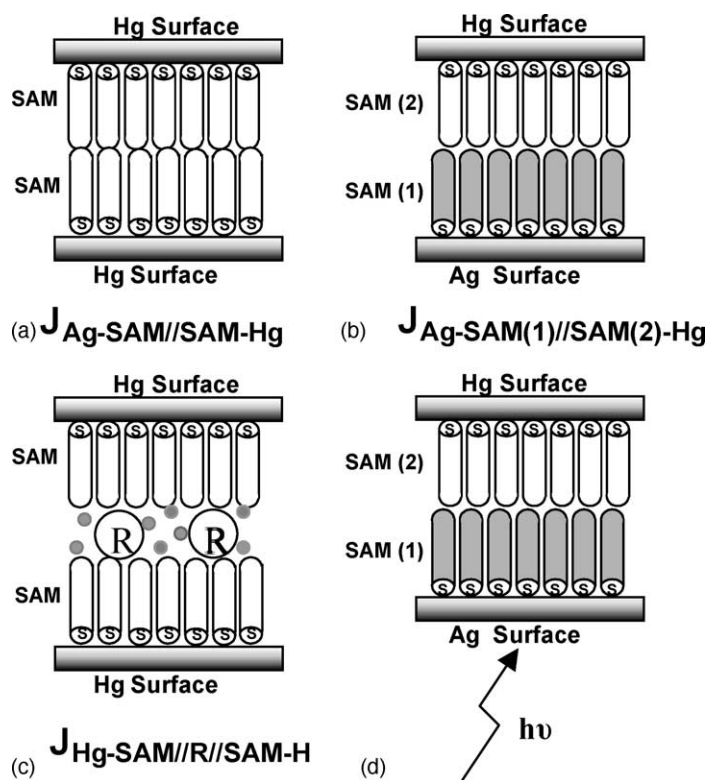


Fig. 2. Schematic representation of the interfaces of the Hg-based junctions: (a) the “liquid–liquid” junction  $J_{\text{Hg-SAM(1)/SAM(2)-Hg}$ ; (b) the “liquid–solid” junction  $J_{\text{Ag-SAM(1)/SAM(2)-Ag}$ ; (c) the “inclusion” junction  $J_{\text{Hg-SAM//R//SAM-Hg}}$  and (d) the junction as photoswitch.

[28]. Recent work on Hg-based junctions is also available by others [54–58].

### 2.1.1. The “liquid–liquid” junction, $J_{\text{Hg-SAM//SAM-Hg}}$ (Fig. 2a)

This junction is formed by bringing two drops of Hg covered by SAMs into contact in a solution of ethanol containing alkanethiol inside a microsyringe (Fig. 3a). Two tungsten wires are inserted into the Hg drops as electrodes.

The “mercury–mercury” junction has the advantage that it uses the same metal (Hg) for the two electrodes, and thus avoids any issue of contamination of the metal used in a solid electrode by mercury through vapor transport. This junction also has several disadvantages: (i) it is difficult to evaluate the contact area; (ii) at high voltages, the facing SAMs may alter their structure by intercalation, compression, spreading, or some other mechanism, as Slowinski and Majda pointed out [24]; (iii) the junction cannot be used with certain types of SAMs (e.g., those generated by polyphenylene-derived thiols).

### 2.1.2. The “liquid–solid” junction, $J_{\text{Hg-SAM(1)/SAM(2)-M}}$ (Fig. 2b)

This junction is formed by using a Hg drop covered by a SAM, and a solid metal surface ( $M$ : Au, Ag, Cu, Pd, Hg/Au alloy) covered by a second SAM (Fig. 3b). The fabrication of these junctions is straightforward: in all cases, the SAMs are

formed separately on the Hg drop and on the solid metal surface. The two metal surfaces covered by SAMs are brought into contact by the use of a micromanipulator in a solution (usually hexadecane) containing the thiol (hexadecanethiol) used to make the SAM on Hg. The presence of this liquid phase (i) protects the mercury drop from vibration; (ii) patches defects created when the SAM covering the Hg drop contacts the solid surface; and (iii) protects the surface of the SAMs from atmospheric contamination.

The SAM on Hg (SAM(1)) and on the solid surface (SAM(2)) can be formed by molecules of different structures (Fig. 2b). The use of a solid surface increases the versatility of the junction substantially, relatively to the liquid–liquid junction, because: (i) on a solid surface it is easy to characterize the organization of the molecules forming the SAM; (ii) the organization of the same molecules can be changed by changing the metal substrate: for example, saturated [59] and conjugated [60] chains form SAMs having different tilt angles on Ag and Au films; (iii) the contact area can be evaluated easily; and (iv) a large range of organic structures can be included in the SAM(2) on the solid surface, and the organization and the structure of these SAMs can be characterized. We have demonstrated that this junction can sustain high electrical fields (6 MV/cm) without electrical breakdown for SAM(2) formed by molecules with very different structures (alkanes, polyphenylene, derivatives of anthracene, and cholesterol) and on the different metals (Ag, Au, Hg, Au/Hg alloy) [28].

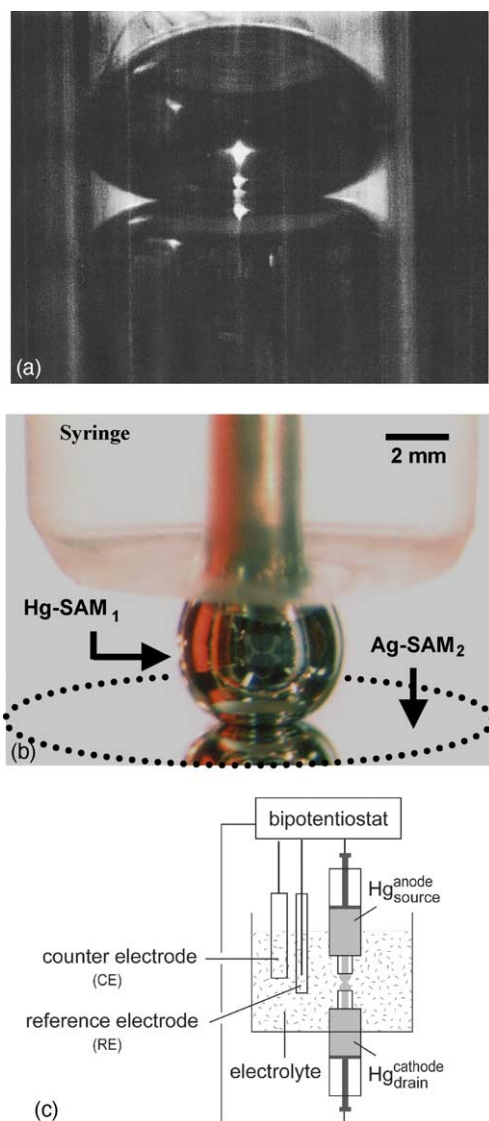


Fig. 3. The Hg-based junctions: (a) photographic images of the  $J_{\text{Hg-SAM}}/\text{SAM-Hg}$  junction: one electrode is inserted into the top Hg drop and the second is inserted into the lower drop, through the syringe needle; (b) photographic image of  $J_{\text{Hg-SAM}(1)}/\text{SAM}(2)\text{-Ag}$  (from [31]); (c) schematic view of a junction containing redox centers either dissolved in the electrolyte ( $J_{\text{Hg-SAM}}/\text{R}/\text{SAM-Hg}$ ) or as part of the SAMs ( $J_{\text{Hg-SAM}}/\text{SAM-Hg}$ ) (from [49]).

### 2.1.3. The “electrochemical inclusion junction”, $J_{\text{Hg-SAM}}/\text{R}/\text{SAM-Hg}$ (Fig. 2c)

In this junction,  $R$  are redox molecules trapped at the interface between the two SAMs. Two-electrode systems suffer from an ambiguity in the relative positions of the Fermi levels of the electrodes with respect to the energy levels of the redox molecules sandwiched between them. In the electrochemical cell represented in Fig. 3c, the junction is immersed in an electrolyte solution, and a macroscopic reference electrode allows potentiostatic control of the energy levels of redox sites trapped in the junction, relative to the potentials applied to the metal electrodes. The electrical neutrality of the solution is provided by lateral movements of ions in the

thin electrolyte film. The SAMs form inert spacers between the mercury electrodes and the layer of electrolyte containing the redox molecules: this spacer permits electron transfer between the electrodes and the redox molecules by tunneling.

### 2.1.4. The junction as photoswitch (Fig. 2d)

For the set-up described in Section 2.1.3, the current passing through the junction can be directly tuned via a gate electrode. It is a crucial step towards devices to couple the electric response of the MIM junction to an external signal. Light can be such a signal, which acts on organic molecules in different ways: It can, for example, induce photoisomerization between configurational isomers (i.e.,  $E$ - and  $Z$ -azobenzene) or constitutional isomers (i.e., photocyclization in diarylethenes [61]), or different electronic states of molecules. A number of publications describe light induced effects on SAMs on surfaces, e.g., photoisomerization [62–66]. With the aim of using light as external signal, we designed and assembled an experimental set-up based on a transparent metal surface as support of a SAM formed by photoactive units (Fig. 2d). This set-up allows both to visualize the contact area between the two SAM-covered electrodes, and to irradiate the SAM through the transparent support (Fig. 4).

### 2.2. Correlation between electrical properties and chemical structure

There is extensive literature discussing electron transfer using molecular systems in solution ( $D$ - $B$ - $A$  systems), where the donor ( $D$ ) and acceptor ( $A$ ) are covalently linked through a molecular bridge ( $B$ ) (Fig. 1a) [67–69]. It is indicated that the rate of electron transfer ( $k_{\text{et}}$ ) depends exponentially on the distance between  $D$  and  $A$  according to Eq. (1), where  $k_{\text{et}}$  is the electron-transfer rate,  $d$  is the length of the bridge, and  $\beta$  is the so-called “decay factor” that correlates the rate of

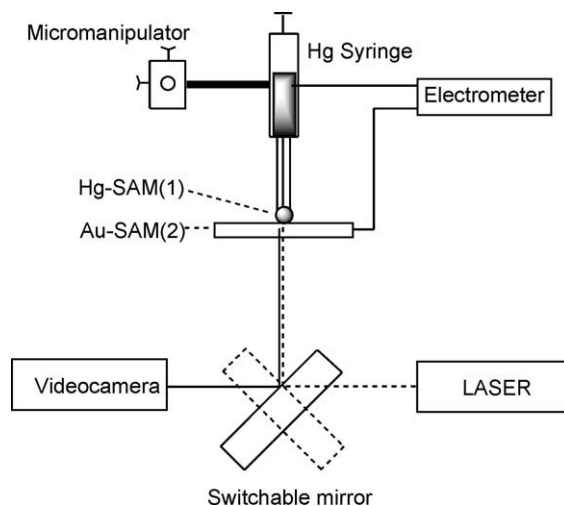


Fig. 4. Schematic set-up of the junction with photoactive units. Through the transparent metal electrode, one can either observe the contact area (switchable mirror in bold position) or irradiate the SAM (switchable mirror in dashed position).

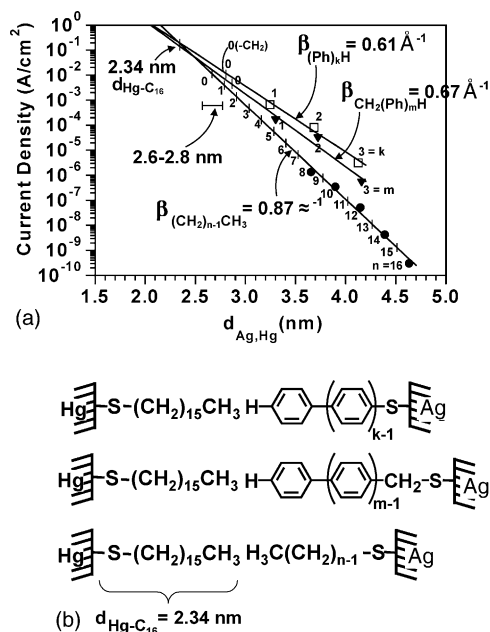


Fig. 5. (a) Plot comparing the distance dependence of current density in  $J_{\text{Hg-C16/SAM(2)-Ag}}$  for SAMs composed of aliphatic thiols  $\text{HS(CH}_2)_{n-1}\text{CH}_3$  (●); oligophenylene thiols  $\text{HS(Ph)}_k\text{H}$  (□); benzylic homologs  $\text{HSCH}_2(\text{Ph})_m\text{H}$  (▼). Current density was obtained at 0.5 V bias. The error in  $\beta$  is  $\sim 0.1 \text{ \AA}^{-1}$ . (b) Schematic representation of junctions formed from the three classes of thiols (Reprinted with permission from [22]. Copyright 2001 American Chemical Society).

electron transfer with the chemical structure of the bridge.

$$k_{\text{et}} = k_0 e^{-\beta d} \quad (1)$$

We have compared rates of electron transfer through saturated and unsaturated molecules of different by measurements of current density, and determined values of  $\beta$  using junctions of the type  $J_{\text{Hg-SAM(1)//SAM(2)-Ag}}$  [22,23].

We have assembled three series of junctions, where SAM(2) was formed from alkanethiols,  $\text{HS(CH}_2)_{n-1}\text{CH}_3$  ( $n = 8, 10, 12, 14, 16$ ), oligophenylene thiols,  $\text{HS(Ph)}_k\text{H}$  ( $k = 1, 2, 3$ ) and benzylic homologs of the oligophenylene thiols  $\text{HSCH}_2(\text{Ph})_m\text{H}$  ( $m = 1, 2, 3$ ) (Fig. 5b). In each junction, SAM(1) was formed from hexadecanethiol. The decrease in current density with increasing length of the molecules forming SAM(2), and therefore with the distance separating the electrodes ( $d_{\text{Ag,Hg}}$ ), followed the relation  $I = I_0 e^{-\beta d_{\text{Ag,Hg}}}$  as expected for tunneling (Fig. 5a). For alkanethiols forming SAM(1) on Ag,  $\beta = 0.87 \pm 0.10 \text{ \AA}^{-1}$ ; for oligophenylene thiols,  $\beta = 0.61 \pm 0.10 \text{ \AA}^{-1}$ ; and for the benzylic derivatives of oligophenylene thiols,  $\beta = 0.66 \pm 0.10 \text{ \AA}^{-1}$ . The values of  $\beta$  are approximately independent of  $V$  (over the range 0.1–1 V).

These values of  $\beta$  are in good agreement with corresponding values obtained by photoinduced electron transfer in molecular  $D$ - $B$ - $A$  systems [67,69–73] and by electron transfer between a solid electrode and redox-active species in solution [8–13]. These results indicate that the information on the “decay factors”  $\beta$  estimated by a wide range of molecular bridges in  $D$ - $B$ - $A$  systems remain fundamen-

tal results for the design of molecular electronic devices [74].

### 3. Redox sites confined inside a junction

“Inclusion junctions”,  $J_{\text{Hg-SAM//R//SAM-Hg}}$ , (Figs. 2c and 3c) allow redox species ( $R$ ) to be sandwiched between the Hg–SAM interface and the potential applied to the two Hg electrodes to be controlled with respect to the potential of  $R$ . We recently reported two different junctions of the type  $J_{\text{Hg-SAM//R//SAM-Hg}}$  [21,31], i.e., with the redox centers dissolved in the electrolyte, and present here a junction of the type  $J_{\text{Hg-SAM//SAM-Hg}}$ , where the redox centers are covalently bound to alkanethiolates and consequently part of the monolayers [49,75]. Fig. 3c shows a schematic illustration of the junction and the associated electrochemical system. The junction consists of two mercury-drop electrodes, both of which support a self-assembled monolayer (SAM) of the ruthenium pentamine pyridine-terminated thiol  $[\text{HS(CH}_2)_{10}\text{CONHCH}_2\text{pyRu(NH}_3)_5](\text{PF}_6)_2$  [10,76]. Cyclic voltammetry of a monolayer in contact with 0.2 M aqueous  $\text{Na}_2\text{SO}_4$  at pH 4 (not shown) shows a redox wave corresponding to the  $\text{Ru}^{\text{II}} \rightleftharpoons \text{Ru}^{\text{III}}$  interconversion at  $E^{\circ'}_{\text{SAM}} = -0.01 \text{ V}$  versus Ag/AgCl, a value that is close to that of a related compound dissolved in the same medium ( $E^{\circ'}_{\text{soln}} = +0.04 \text{ V}$  versus SCE [10]).

We studied electron transport across the Hg–SAM//SAM–Hg junction by placing the junction, together with a Ag/AgCl reference electrode and a platinum counter electrode, in a pH 4  $\text{Na}_2\text{SO}_4$  electrolyte solution, and by using a bipotentiostat that allowed the potentials of the mercury electrodes to be controlled independently with respect to the reference electrode (Fig. 3c). The potentials of the mercury electrodes were controlled such that one (cathode) acted as electron donor and the other (anode) as electron acceptor. We designated the cathode and anode as the drain and source electrodes, respectively, by analogy to the convention used in semiconductor devices, where current is considered to flow from a more positive region to a more negative region [76]. We measured the conductance through the junction as a function of the potentials of the drain and source electrodes with respect to the reference electrode (i.e.,  $V_{\text{DG}}$  and  $V_{\text{SG}}$ , respectively) and as a function of the potential between the source and drain ( $V_{\text{DS}}$ ), using the electrolyte solution as a gate [77]. We controlled the potential of the gate by tuning the potential applied to the reference electrode relative to ground. Since the source electrode is grounded, this voltage is  $V_{\text{SG}}$ .

Fig. 6a shows the drain/source currents when  $V_{\text{DG}}$  is fixed at  $-0.20 \text{ V}$ , where the attached ruthenium is in its +2 oxidation state, and  $V_{\text{SG}}$  is varied. For  $V_{\text{SG}} \leq V_{\text{DG}}$ , the currents are negligible and the junction is non-conducting. Increasing  $V_{\text{SG}}$  to values more positive than  $-0.14 \text{ V}$  results in an anodic current flow corresponding to the oxidation of  $\text{Ru}^{\text{II}}$  to  $\text{Ru}^{\text{III}}$  at the source and a cathodic current flow corresponding to the reduction of  $\text{Ru}^{\text{III}}$  to  $\text{Ru}^{\text{II}}$  at the drain. The anodic

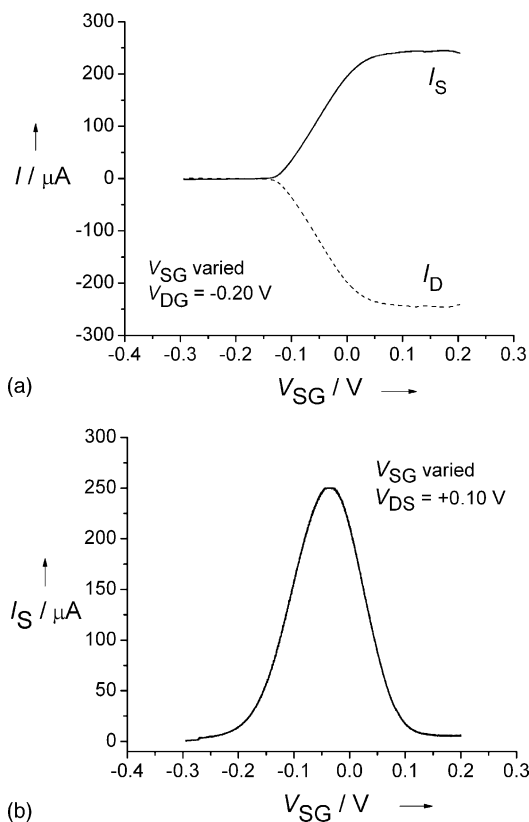


Fig. 6. Current–voltage characteristics of the Hg–SAM//SAM–Hg junction, showing diode- and transistor-like behavior. All experiments were carried out in 0.2 M aqueous  $\text{Na}_2\text{SO}_4$  at pH 4. (a)  $I_D$  and  $I_S$  as a function of  $V_{SG}$ .  $V_{DG}$  was fixed at  $-0.20$  V and scan rate was 50 mV/s. (b)  $I_S$  as a function of  $V_{SG}$  for the same junction as in (A).  $V_{DS}$  was fixed at  $+0.10$  V.  $I_D$  (not shown) is equal in magnitude but opposite in sign to  $I_S$ ; the scan rate was 10 mV/s (Reprinted with permission from [49]. Copyright 2004 WILEY-VCH.).

and cathodic currents are equal and increase to a plateau with a half-wave (half-maximum) potential,  $-0.04$  V, that is near the formal potential,  $E^\circ$ , of the  $\text{Ru}^{\text{II/III}}$  couple. For an electrode contact area of  $\sim 0.20$  mm<sup>2</sup>, the maximum current passing through the electrodes is typically about 1.3 mA/mm<sup>2</sup> (or 1000 electrons/second/molecule), a value that is approximately 600-fold higher than that observed when only one of the mercury electrodes is electrically connected to the bipotentiostat.

In Fig. 6b, we show the conductance of the Hg–SAM//SAM–Hg junction operating at fixed drain-source potentials. Fig. 6b shows that at fixed  $V_{DS} = +0.10$  V, the drain current is negligible for  $V_{SG}$  less than  $-0.25$  V and greater than  $+0.15$  V. Upon scanning  $V_{SG}$  from  $-0.25$  to  $+0.15$  V, the current increases from zero to a maximum value near the  $E^\circ$  of the redox couple and then decreases again to zero. Charge therefore passes from one electrode to another only when  $V_{SG}$  is at or close to the  $\text{Ru}^{\text{II/III}}$  redox potential.

Based on these observations, we propose that charge transport through the junction occurs as a result of oxidation of  $\text{Ru}^{\text{II}}$  to  $\text{Ru}^{\text{III}}$  at the source, electron exchange between  $\text{Ru}^{\text{III}}$  at the source and  $\text{Ru}^{\text{II}}$  at the drain, and reduction of

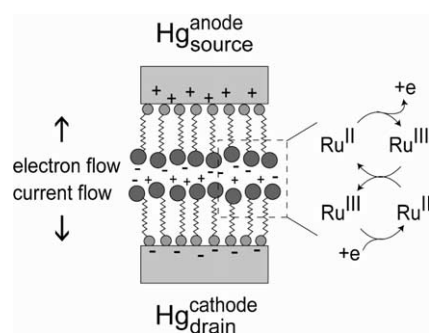


Fig. 7. Schematic diagram of the proposed mechanism of charge transport through the Hg–SAM//SAM–Hg junction, when  $V_{SG}$  is swept from negative to positive potentials and  $V_{DG} \leq -0.14$  V (Reprinted with permission from [49]. Copyright 2004 WILEY-VCH.).

$\text{Ru}^{\text{III}}$  at the drain back to  $\text{Ru}^{\text{II}}$  as key steps (Fig. 7). Similar surface-to-surface charge transport mechanisms have been reported previously for a variety of interfaces including polymer/polymer [78,79] and polymer/electrolyte solution [80]; such electron transport processes, however, have not been reported for molecular monolayers.

This junction shows electrical behavior similar to that of a solid-state transistor when the electrolyte is used as the gate. It is less stable than conventional FETs (field effect transistors), but easy to assemble and to modify.

#### 4. Conclusions

The junctions Hg–SAM//SAM–Hg, Hg–SAM//SAM–metal, Hg–SAM//R//SAM–Hg are the basis for a new, physical–organic-based approach to the study of electron transport in organic nm-thick films. These systems and junctions have advantages and disadvantages relative to other systems for studying electron transport.

The results obtained with these Hg–SAM-based junctions provide a new experimental approach to the measurement and comparison of electron-transport rates (i) across a large variety of organic and organometallic ordered thin films; (ii) across different kinds of chemical bonds [23]; (iii) across nm-scale gaps in processes mediated by redox molecules as electron carriers and (iv) through photoactive molecules. The results we have obtained in all of the systems examined to date indicate that the mechanism of electron transport is tunneling between the metal junctions across the SAMs. For some molecules, however, controlling the potential of the two electrodes can cause an orbital (usually the HOMO or LUMO) of the molecule to fall between the Fermi levels of the electrodes, causing a change in the transport process from “tunneling” to “hopping”.

We believe that the results obtained in this work indicate that these junctions are systems that can be used to collect reliable experimental data on the electrical behavior of a wide variety of molecular systems. They represent a useful complement to physics-based experimental methods. We hope that

they will contribute to the understanding of electron transport in mesoscale systems, and to the design of molecular electronic devices.

## Acknowledgments

This work was supported by the ONR, DARPA, and the NSF (ECS-9729405) (USA), by the CNR (Italy) and the European Union (Grants G5RD-CT-2002-00776 MWFM and IST-2001-35503 LIMM).

## References

- [1] V. Balzani (Ed.), *Electron Transfer in Chemistry*, vol. I–V, Wiley, Weinheim, 2001.
- [2] B. Mann, H. Kuhn, *J. Appl. Phys.* 42 (1971) 4398.
- [3] A. Aviram, M.A. Ratner, *Chem. Phys. Lett.* 29 (1974) 277.
- [4] H.D. Sikes, J.F. Smalley, S.P. Dudek, A.R. Cook, M.D. Newton, C.E.D. Chidsey, S.W. Feldberg, *Science* 291 (2001) 1519.
- [5] E.P.A.M. Bakker, A.L. Roest, A.W. Marsman, L.W. Jenneskens, L.I. De Jong-van Steensel, J.J. Kelly, D. Vanmaekelberg, *J. Phys. Chem. B* 104 (2000) 7266.
- [6] S. Creager, C.J. Yu, C. Bamdad, S. O'Connor, T. MacLean, E. Lam, Y. Chong, G.T. Olsen, J. Luo, M. Gozin, J.F. Kayyem, *J. Am. Chem. Soc.* 121 (1999) 1056.
- [7] S.B. Sachs, S.P. Dudek, R.P. Hsung, L.R. Sita, J.F. Smalley, M.D. Newton, S.W. Feldberg, C.E.D. Chidsey, *J. Am. Chem. Soc.* 119 (1997) 10563.
- [8] K. Slowinski, R.V. Chamberlain, C.J. Miller, M. Majda, *J. Am. Chem. Soc.* 119 (1997) 11910.
- [9] K. Weber, L. Hockett, S. Creager, *J. Phys. Chem. B* 101 (1997) 8286.
- [10] H.O. Finklea, D. Hanshaw, *J. Am. Chem. Soc.* 114 (1992) 3173.
- [11] J.F. Smalley, S.W. Feldberg, C.E.D. Chidsey, M.R. Lindford, M. Newton, Y.-P. Liu, *J. Phys. Chem.* 99 (1995) 13141.
- [12] A.M. Becka, C.J. Miller, *J. Phys. Chem.* 96 (1992) 2657.
- [13] C.E.D. Chidsey, *Science* 251 (1991) 919.
- [14] Y. Xia, J.A. Rogers, K.E. Paul, G.M. Whitesides, *Chem. Rev.* 99 (1999) 1823.
- [15] R. Weisendanger, *Scanning Probe Microscopy and Spectroscopy*, Cambridge University Press, Cambridge, 1994.
- [16] A. Ulman, *Chem. Rev.* 96 (1996) 1533.
- [17] R.M. Metzger, T. Xu, I. Petersen, *J. Phys. Chem.* 105 (2001) 7280.
- [18] X.D. Cui, A. Primak, X. Zarate, J. Tomfohr, O.F. Sankey, A.L. Moore, T.A. Moore, D. Gust, G. Harris, S.M. Lindsay, *Science* 294 (2001) 571.
- [19] Z.J. Donhauser, B.A. Mantooth, K.F. Kelly, L.A. Bumm, J.D. Monnell, J.J. Stapleton, D.W. Price Jr., A.M. Rawlett, D.L. Allara, J.M. Tour, P.S. Weiss, *Science* 292 (2001) 2303.
- [20] H.J. Park, A.K.L. Lim, E.H. Anderson, A.P. Alivisatos, P.L. McEuen, *Nature* 407 (2000) 680.
- [21] M.L. Chabinyc, X. Chen, R.E. Holmlin, H. Jacobs, H. Skulason, C.D. Frisbie, V. Mujica, M.A. Ratner, M.A. Rampi, G.M. Whitesides, *J. Am. Chem. Soc.* 124 (2002) 11730.
- [22] R.E. Holmlin, R. Haag, R.F. Ismagilov, M.A. Rampi, G.M. Whitesides, *J. Am. Chem. Soc.* 123 (2001) 5075.
- [23] R.E. Holmlin, R.F. Ismagilov, R. Haag, V. Mujica, M.A. Ratner, M.A. Rampi, G.M. Whitesides, *Angew. Chem. Int. Engl. Ed.* 40 (2001) 2316.
- [24] K. Slowinski, M. Majda, *J. Electroanal. Chem.* 491 (2000) 13.
- [25] J.K. Gimzewski, C. Joachim, *Science* 283 (1999) 1683.
- [26] J. Chen, M.A. Reed, A.M. Rawlett, J.M. Tour, *Science* 286 (1999) 1550.
- [27] K. Slowinski, H.K.Y. Fong, M. Majda, *J. Am. Chem. Soc.* 103 (1999) 7257.
- [28] R. Haag, M.A. Rampi, R.E. Holmlin, G.M. Whitesides, *J. Am. Chem. Soc.* 103 (1999) 7895.
- [29] M.A. Rampi, O.J. Schueller, G.M. Whitesides, *Appl. Phys. Lett.* 72 (1998) 1781.
- [30] D. Poraths, A. Bezryadin, S. De Vries, C. Dekker, *Nature* 403 (2000) 635.
- [31] M.A. Rampi, G.M. Whitesides, *Chem. Phys.* 281 (2002) 373.
- [32] J.M. Beebe, V.B. Engelkes, L.L. Miller, C.D. Frisbie, *J. Am. Chem. Soc.* 124 (2002) 11268.
- [33] J. Reichert, R. Ochs, D. Beckmann, H.B. Weber, M. Mayor, H. van Löhneysen, *Phys. Rev. Lett.* 88 (2002) 176804.
- [34] Y. Selzer, A. Salomon, D. Cahen, *J. Phys. Chem. B* 106 (2002) 10432.
- [35] A. Vilan, A. Shanzer, D. Cahen, *Nature* 404 (2000) 166.
- [36] W.Y. Wang, T. Lee, M.A. Reed, *Phys. Rev. B* 68 (2003) 035416.
- [37] B. de Boer, M.M. Frank, Y.J. Chabal, W. Jiang, E. Garfunkel, Z. Bao, *Langmuir* 20 (2004) 1539.
- [38] Y.-L. Loo, D.V. Lang, J.A. Rogers, J.W.P. Hsu, *Nano Lett.* 3 (2003) 913.
- [39] C.M. Wynn, T.H. Fedynyshyn, M.W. Geis, R.R. Kunz, T.M. Lyszczarz, M. Rothschilds, S.J. Spector, M. Switkes, *Nanotechnology* 15 (2004) 86.
- [40] J.G. Kushmerick, J. Naciri, J.C. Yang, R. Shashidhar, *Nano Lett.* 3 (2003) 897.
- [41] Y. Liu, X. Fan, D. Yang, C. Wang, L. Wan, C. Bai, *Langmuir* 20 (2004) 855.
- [42] L.T. Cai, H. Skulason, J.G. Kushmerick, S.K. Pollack, J. Naciri, R. Shashidhar, D.L. Allara, T.E. Mallouk, T.S. Mayer, *J. Phys. Chem. B* 108 (2004) 2827.
- [43] W. Haiss, H. van Zalinge, S.J. Higgins, D. Bethell, H. Höbenreich, D.J. Schiffrin, R.J. Nichols, *J. Am. Chem. Soc.* 125 (2003) 15295.
- [44] R.A. Wassel, G.M. Credo, R.R. Fruierer, D.L. Feldheim, C.B. Gorman, *J. Am. Chem. Soc.* 126 (2004) 295.
- [45] G.K. Ramachandran, T.J. Hopson, A.M. Rawlett, L.A. Nagahara, A. Primak, S.M. Lindsay, *Science* 300 (2003) 1413.
- [46] X. Xiao, B. Xu, N.J. Tao, *Nano Lett.* 4 (2004) 267.
- [47] M. Mayor, H.B. Weber, J. Reichert, M. Elbing, C. von Hänisch, D. Beckmann, M. Fischer, *Angew. Chem. Int. Ed.* 42 (2003) 5834.
- [48] S. Lenfant, C. Krzeminski, C. Delerue, G. Allan, D. Vuillaume, *Nano Lett.* 3 (2003) 741.
- [49] E. Tran, M.A. Rampi, G.M. Whitesides, *Angew. Chem. Int. Ed.* 43 (2004) 3835.
- [50] O.M. Magnussen, B.M. Ocko, M. Deutsch, M.J. Regan, P.S. Pershan, L.E. Berman, D. Abernathy, J.F. Legrand, G. Grubel, *Nature* 384 (1996) 250.
- [51] A. Demoz, D.J. Harrison, *Langmuir* 9 (1993) 1046.
- [52] C. Bruckner-Lea, R.J. Kimmel, J. Janata, J.F.T. Conroy, K. Caldwell, *Electrochim. Acta* 40 (1995) 2897.
- [53] K. Slowinski, R.V. Chamberlain II, R. Bilewicz, M. Majda, *J. Am. Chem. Soc.* 118 (1996) 4709.
- [54] S. Sek, R. Bilewicz, K. Slowinski, *Chem. Commun.* (2004) 404.
- [55] N.K. Chaki, M. Aslam, T.G. Gopakumar, J. Sharma, R. Pasricha, I.S. Mulla, K. Vijayamohan, *J. Phys. Chem. B* 107 (2003) 13567.
- [56] M. Galperin, A. Nitzan, S. Sek, M. Majda, *J. Electroanal. Chem.* 550–551 (2003) 337.
- [57] R.L. York, K. Slowinski, *J. Electroanal. Chem.* 550–551 (2003) 327.
- [58] Y. Selzer, A. Salomon, J. Ghabboun, D. Cahen, *Angew. Chem. Int. Ed.* 41 (2002) 827.
- [59] P.E. Laibinis, B.J. Palmer, S.W. Lee, G.K. Jennings, *Thin Solid Films* 24 (1998) 1.
- [60] S. Frey, V. Stadler, K. Heister, W. Eck, M. Zharnikov, M. Grunze, B. Zeysing, A. Terfort, *Langmuir* 17 (2001) 2408.
- [61] M. Irie, *Chem. Rev.* 100 (2000) 1685.

- [62] S.D. Evans, S.R. Johnson, H. Ringsdorf, L.M. Williams, H. Wolf, *Langmuir* 14 (1998) 6436.
- [63] D.G. Walter, D.J. Campbell, C.A. Mirkin, *J. Phys. Chem. B* 103 (1999) 402.
- [64] D. Gustina, E. Markava, I. Muzikante, B. Stiller, L. Brehmer, *Adv. Mater. Opt. Electron.* 9 (1999) 245.
- [65] H. Akiyama, K. Tamada, J. Nagasawa, K. Abe, T. Tamaki, *J. Phys. Chem. B* 107 (2003) 130.
- [66] S. Yasuda, T. Nakamura, M. Matsumoto, H. Shigekawa, *J. Am. Chem. Soc.* 125 (2003) 16430.
- [67] M.N. Paddon-Row, in: V. Balzani (Ed.), *Electron Transfer in Chemistry*, vol. III, Wiley-VCH, Weinheim, 2001, p. 179.
- [68] D. Guest, T.M. Moore, A.L. Moore, in: V. Balzani (Ed.), *Electron Transfer in Chemistry*, vol. III, Wiley-VCH, Weinheim, 2001, p. 272.
- [69] F. Scandola, C. Chorboli, M.T. Indelli, M.A. Rampi, in: V. Balzani (Ed.), *Electron Transfer in Chemistry*, vol. III, Wiley-VCH, Weinheim, 2001, p. 337.
- [70] J.W. Verhoeven, J. Kroon, M.N. Paddon-Row, A.M. Oliver, in: D.O. Hall, G. Grassi (Eds.), *Photoconversion Processes for Energy and Chemicals*, Elsevier, 1989, p. 100.
- [71] M.N. Paddon-Row, *Acc. Chem. Res.* 27 (1994) 18.
- [72] A. Helms, D. Heiler, G. McLendon, *J. Am. Chem. Soc.* 114 (1992) 6227.
- [73] M. Staffilani, P. Belser, F. Hartl, C.J. Kleverlaan, L. De Cola, *J. Phys. Chem. A* 106 (2002) 9242.
- [74] A. Salomon, D. Cahen, S. Lindsay, J. Tomfohr, V.B. Engelkes, C.D. Frisbie, *Adv. Mater.* 15 (2003) 1881.
- [75] For analysis of the electron transport properties of this system, see: W. Schmickler, M.A. Rampi, E. Tran, G.M. Whitesides, *Faraday Discuss.* 125 (2004) 171.
- [76] P. Horowitz, H. Winfield, *The Art of Electronics*, Cambridge University Press, New York, 1995.
- [77] The use of an electrolyte as a gate electrode and the reference electrode to establish the gate potential is called electrochemical gating. The operating principle of this technique is that the Fermi energy of the source and drain electrodes can be raised or lowered by controlling their potentials with respect to the reference electrode. For example, driving the source electrode to more positive potentials (with respect to the reference) lowers the Fermi energy and hence the energy of the electrons within the electrode. The positive charge on the source electrode is balanced by anions in the electrolyte. The presence of excess electrolyte anions, in turn, raises the orbital energy of the surface-bound redox species. Oxidation of the redox species ensues when the potential of the source electrode reaches a level positive enough to accept an electron from the redox species.
- [78] G.P. Kittlesen, H.S. White, M.S. Wrighton, *J. Am. Chem. Soc.* 107 (1985) 7373.
- [79] P.G. Pickup, W. Kutner, C.R. Leidner, R.W. Murray, *J. Am. Chem. Soc.* 106 (1984) 1991.
- [80] T. Ikeda, C.R. Leidner, R.W. Murray, *J. Am. Chem. Soc.* 103 (1981) 7422.